40CrMoV13.9 notched specimens under multiaxial fatigue: an overview of recent results

S.M.J. Razavi, M. Peron, J. Torgersen, F. Berto, T. Welo
Department of Mechanical and Industrial Engineering, Norwegian University of Science and Technology (NTNU), Norway
javad.razavi@ntnu.no, mirco.peron@ntnu.no, jan.torgersen@ntnu.no, filippo.berto@ntnu.no

ABSTRACT. The multiaxial fatigue strength of circumferentially V-notched and semicircular notched specimens made of 40CrMoV13.9 has been investigated in this paper. The multiaxial load were applied using combined tension and torsion loading, both in-phase and out-of-phase. The axis-symmetric V-notched specimens were characterized by a blunt notch tip (radius: 1 mm) and notch opening angle of 90° and the semicircular specimens were characterized by a constant notch tip radius. The net sectional area of both cases was equal with a diameter of 12 mm. The notched specimens were tested under pure mode I (tension), mixed mode I/III and pure mode III (torsion). More than 120 fatigue test data are used in this paper to evaluate the fatigue behaviour of 40CrMoV13.9 alloy. All fatigue data are analysed using the Average Strain Energy Density (ASED) criterion which employs the mean value of the strain energy density evaluated over a finite size semicircular sector surrounding the tip of the notch to predict the fatigue life of the tested specimens.

KEYWORDS. Multiaxial fatigue; SED criterion; Notched components; Mixed mode I/III.

Citation: Razavi, S.M.J., Peron, M., Torgersen, J., Berto, F., Welo, T., 40CrMoV13.9 notched specimens under multiaxial fatigue: an overview of recent results, Frattura ed Integrità Strutturale, 41 (2017) 440-446.

Received: 18.05.2017
Accepted: 27.05.2017
Published: 01.07.2017

INTRODUCTION

The majority of engineering components are subjected to complex multiaxial loading histories. This makes it especially important to be able to accurately estimate fatigue damage under multiaxial loading. To this end, considerable effort in the past decades has been put into developing damage parameters which reflect the actual damage mechanisms of the multiaxial fatigue failure process [1-6]. Numerous predictive methods have been proposed in the literature for the cracked and notched components under multiaxial loading including the critical plane [7,8], energetic criterion [9] and thermodynamics based method [10]. Nieslony and Sonsino [11] conducted a comparison among different available failure criteria considering a large bulk of experimental data from notched specimens. Ayatollahi et al. [12] proposed a local numerical method in order to predict the fatigue crack initiation and propagation in the cracked and

notched components. This method was then enhanced by other scholars to consider different parameters which affect the fatigue crack growth behaviour in different materials [13-19].
Prediction of the branch crack threshold condition under mixed mode (I+III) was suggested by Pook and Sharples [20] through the analysis of the main crack tip stress field. Pook [21] revealed that there are different thresholds for the initiation of crack growth, crack arrest and specimen failure under multiaxial fatigue loading. Additionally, definition of a fatigue threshold ΔK_{th} under poly-modal loading is difficult because under torsion loading an extensive plastic zone is developed at the vicinity of the crack [22]. The presence of plastic deformation around the crack tip in conjunction with the dissipative phenomena due to the possible contact of the crack surfaces result in a strong influence of the specimen geometry on the test data. Christopher et al. [23] developed a novel mathematical model of the stress fields around the crack tip under fatigue loading, taking into account the effects of plasticity through an analysis of their shielding effects on the applied elastic field. Lin et al. [24] studied the complex initiation of crack growth under a combination of opening and out of plane shearing mode loading showing that the cracks do not grow through a continuous evolution of the crack surface but rather by means of an abrupt fragmentation or segmentation of the crack front.
In the last years the ASED approach which is based on the average value of strain energy density over a control volume has been extended for various brittle and quasi-brittle materials under tensile loading and a wide range of materials under fatigue loading. In particular, this method was used to assess the fatigue behaviour of axisymmetric specimens made of a medium carbon steel (C40) [25] and a 39NiCrMo3 [26] steel subjected to uniaxial and multiaxial loading. In addition, the dissipative phenomena and non-propagating cracks in the run-out specimens were studied by Berto et al. [27] and [28]. They reported that the control volume radius was found to be strongly influenced by extrinsic shielding mechanisms under mode III loading conditions.
In the current paper, the multiaxial fatigue strength of circumferentially V-notched and semicircular notched specimens made of 40CrMoV13.9 were investigated under combined tension and torsion loading. The ASED criterion is used in order to predict the fatigue strength of notched components subjected to uniaxial and multiaxial loading. For 40CrMoV13.9 alloy which is a high strength steel the ASED approach is essentially able to overcome the complexity of non-proportional loading using a single control volume which was used independent of the loading mode.

MATERIAL AND GEOMETRY OF THE SPECIMENS

All the specimens were made of 40CrMoV13.9 steel. Static tensile tests were carried out to evaluate the elastic and the strength properties of the material; the relevant mean values are listed in Tab. 1, while the chemical composition of the material is reported in Tab. 2.

Ultimate tensile strength (MPa)	Yield stress (MPa)	Elongation to fracture (%)	Brinell Hardness
1355	1127	15.2	393-415

Table 1: Mechanical properties of 40CrMoV13.9.

C	Mn	Si	S	P	Cr	Ni	Mo	V	Al	W
0.38	0.5	0.27	0.006	0.003	3.05	0.24	1.04	0.24	0.013	0.005

Table 2: Chemical composition wt.%, balance Fe.

The geometries of the specimens tested in the present investigation are shown in Fig. 1. The V-notch depth d was equal to 4 mm for both cases. The axis-symmetric V-notched specimens were characterized by a constant notch tip radius (1 mm) and a V-notch opening angle equal to 90°. The geometry of semicircular specimens instead was characterized by a constant notch tip radius equal to 4 mm.

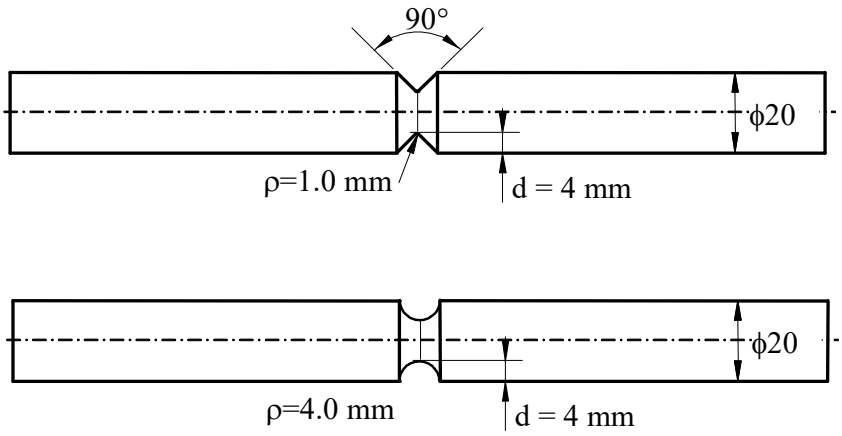

Figure 1: Geometry of V-notched specimens and semicircular specimens.

The specimens were tested under pure tension, pure torsion and multiaxial tension-torsion loading with different biaxiality ratios ($\lambda = \tau_a/\sigma_a$ =0.6 and 1.0). In particular, ten fatigue test series were conducted, according to the following subdivision:

1) Two series of tests on notched specimens (V and semicircular notches) under pure torsion fatigue loading (nominal load ratio R = -1);
2) One series of tests on V-notched specimens under pure tension fatigue loading (nominal load ratio R = -1).
3) Two series of tests on V-notched specimens under combined tension-torsion fatigue loading, under constant biaxiality ratio λ = 1, load ratio R = -1, load phase angle φ= 0° or φ= 90°;
4) Two series of tests on V-notched specimens under combined tension-torsion fatigue loading, under constant biaxiality ratio λ = 0.6, load ratio R = -1, load phase angle φ= 0° or φ= 90°;
5) Two series of tests on semicircular specimens under combined tension-torsion fatigue loading, under constant biaxiality ratio λ = 1, load ratio R = -1, load phase angle φ= 0° or φ= 90°;
6) One series of tests on semicircular specimens under combined tension-torsion fatigue loading, under constant biaxiality ratio λ = 0.6, load ratio R = -1, load phase angle φ= 0°.

FATIGUE TEST DATA ON V-NOTCHED AND SEMICIRCULAR SPECIMENS

Before being tested, all specimens have been polished in order to both eliminate surface scratches or machining marks and to make the observation of the fatigue crack path easier. Fatigue tests have been carried out on a MTS 809 servo-hydraulic biaxial machine with a 100 kN axial load cell and a torsion load cell of 1100 N.m. All tests have been performed under load control, with a frequency ranging from 1 and 10 Hz, as a function of the geometry and load level. At the end of the fatigue tests, the notch root and the fracture surfaces were examined using optical and electronic microscopy. Some examples of fracture surfaces are visible in Fig. 2a and 2b for in phase and out of phase multiaxial loading.

The results of statistical analyses carried out by assuming a log-normal distribution are summarised in Tab. 3. In particular, it is summarised the mean values of the nominal stress amplitudes at different number of cycles, the inverse slope k of the Wöhler curves and the scatter index T, which quantifies the width of the scatterband included between 10 and 90% probability of survival curves. All failures from 10^4 to $5x10^6$ have been processed in the statistical analysis whereas the run-outs were excluded.

Fig. 3 depicts fatigue data from V-notched specimens tested under tension, torsion and combined tension and torsion with different load phases. In this case the biaxiality ratio is equal to 1. It is visible from the figure that the out of phase loading causes a detrimental effect on the fatigue life of the V-notched specimens. This effect is not observed in the case of semicircular notches where the most damaging case is the in-phase loading. By changing the biaxiality ratio from 1 to 0.6 on V notched specimens tests, the effect of out of phase is again present. Summarising this aspect it seems that the phase displacement could increase or vice versa decrease the fatigue life of the component as a function of the notch geometry.

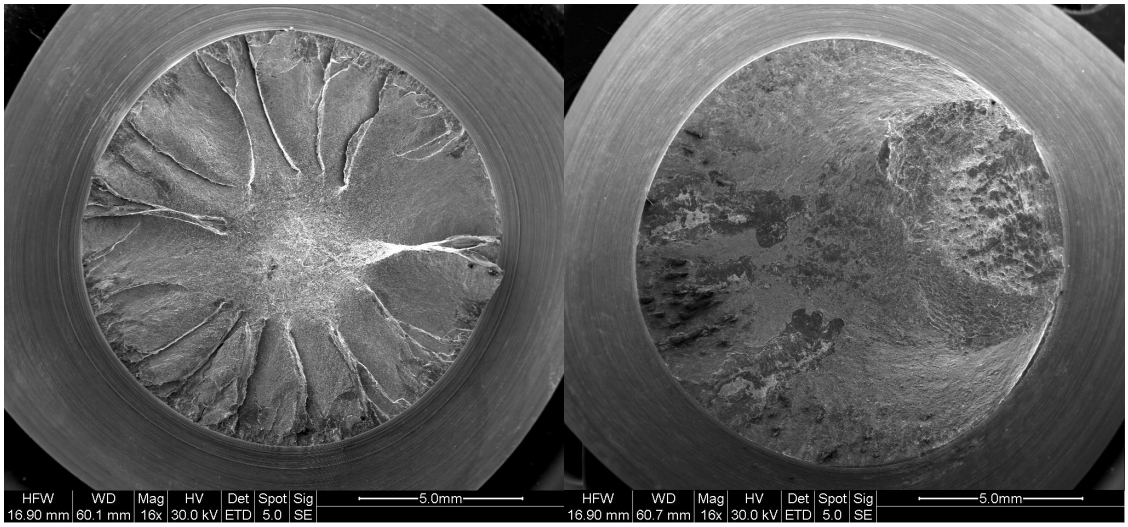

Figure 2: Fracture surfaces of (a) in phase and (b) out of phase multiaxial loading.

Series	Load	N		k	T_σ or T_τ	σ_a or τ_a		
						10^6	$2\ 10^6$	$5\ 10^6$
1	Torsion R = -1	16	τ	13.33	1.144	281.16	266.91	249.18
2	Multiaxial R = -1, φ= 0°, λ = 1.0	14	σ	9.39	1.176	182.6	169.91	153.84
3	Multiaxial R = -1, φ= 90°, λ = 1.0	13	σ	7.67	1.428	145.83	133.23	118.23
4	Tension R = -1	12	σ	8.42	1.335	253.69	233.64	209.55
5	Multiaxial R = -1, φ = 0°, λ = 0.6	12	σ τ	9.9	1.202	214.61 128.77	200.10 120.06	182.41 109.45
6	Multiaxial R = -1, φ = 90°, λ = 0.6	13	σ τ	7.63	1.485	187.45 112.47	171.17 102.7	151.8 91.08
7	Torsion R = -1 Semicircular	11	τ	14.27	1.160	367.17	349.76	328.01
8	Multiaxial R = -1, φ = 0°, λ = 1.0 Semicircular	15	σ	7.68	1.268	239.57	218.9	194.28
9	Multiaxial R = -1, φ = 90°, λ = 1.0 Semicircular	17	σ	10.79	1.260	263.82	247.4	227.26
10	Multiaxial R = -1, φ = 0°, λ = 0.6 Semicircular	12	σ τ	11.45	1.307	332.64 199.58	313.10 187.86	289.02 173.41

Table 3: Results from fatigue tests. Mean values, Ps=50%. Stresses referred to the net area.

A SYNTHESIS IN TERMS OF LINEAR ELASTIC SED AVERAGED OVER A CONTROL VOLUME

The averaged strain energy density criterion (SED) states that brittle failure occurs when the mean value of the strain energy density over a given control volume is equal to a critical value W_c. This critical value varies from material to material but does not depend on the notch geometry and sharpness. In the particular case of 40CrMoV13.9 steel the radius of the control volume (R_c) has been found to be equal to 0.05 mm. Dealing with V-shaped notches the control volume is defined as is visible in Fig. 4a, the volume assumes a crescent shape and it is centred at a distance equal to r_0 from the notch tip. The distance r_0 depends on the radius of the notch ϱ and on the notch opening angle 2α.

$$q = \frac{2\pi - 2\alpha}{\pi} \tag{1}$$

$$r_0 = \frac{q-1}{q}\rho \tag{2}$$

For semicircular notches under mode I and III loadings, the volume assumes the crescent shape shown in Fig. 4b, where Rc is the depth measured along the notch bisector line. The outer radius of the crescent shape is equal to $R_c+\varrho/2$, being $\varrho/2$ the distance between the notch tip and the origin of the local coordinate system.

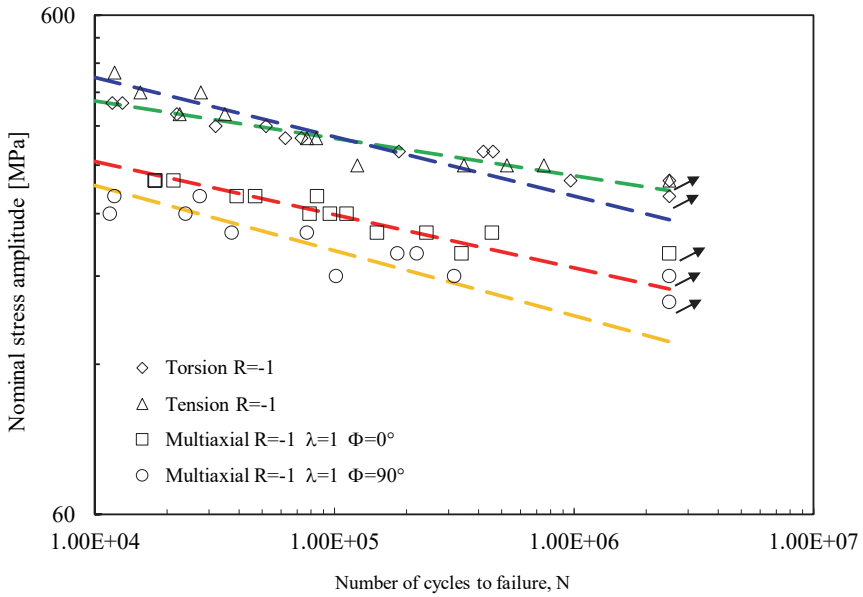

Figure 3: Data from multiaxial tests from V-notched specimens.

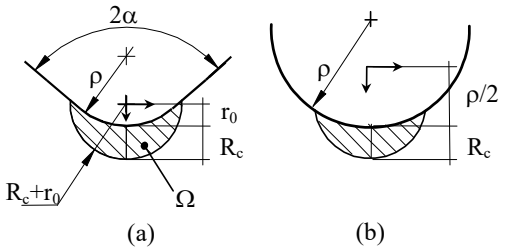

Figure 4: Critical volume for (a) V-shaped notches and (b) semicircular notches.

The value of the SED averaged over the control volume carefully defined as presented above, has been calculated numerically by using the FE code ANSYS 12.0® both for V-notched and semicircular notched specimens. Fig. 5 shows the synthesis based on local SED. By comparing Fig. 5 with Fig. 3 it is evident that a single narrow scatterband has been obtained by means of the local energy.

Conclusions

A large bulk of results from multiaxial tests on V-notched and semicircular notched specimens made of 40CrMoV13.9 steel are discussed together with those obtained under pure tension and pure torsion loading from notched specimens with the same geometry. Altogether more than 120 new fatigue data (10 fatigue curves) are

summarised in the present work.
All fatigue data are present first in terms of nominal stress amplitudes and then re analysed in terms of the mean value of the strain energy density evaluated over a finite size semicircular sector surrounding the tip of the notch. The synthesis permits to obtain a very narrow band characterised by a scatter index equal to 1.96. The synthesis has been carried out with a constant radius independent on the loading conditions.

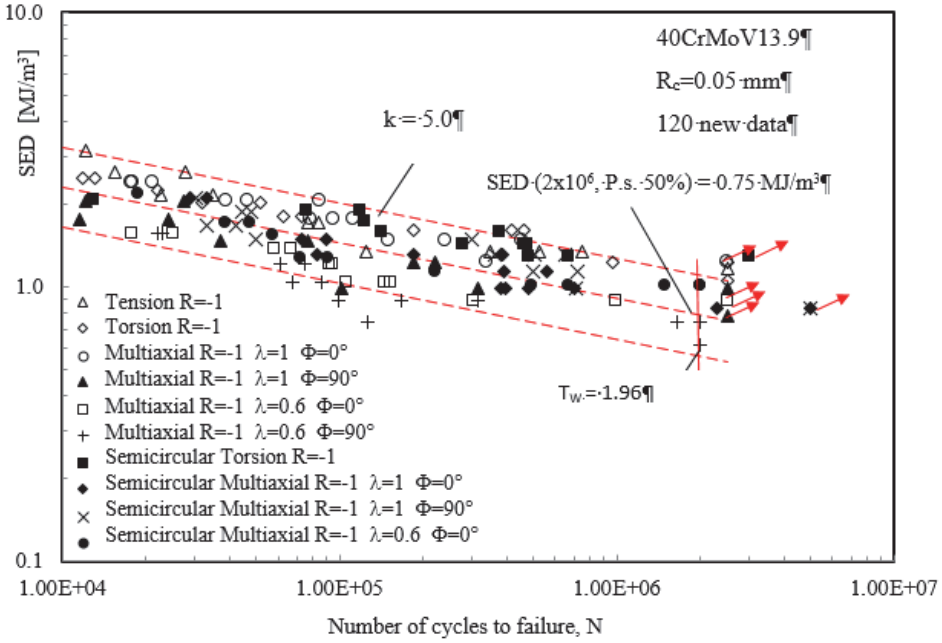

Figure 5: Synthesis by means of local SED of multiaxial series data.

REFERENCES

[1] Gates, N.R., Fatemi, A., Interaction of shear and normal stresses in multiaxial fatigue damage analysis, Frattura ed Integrita Strutturale, 10(37) (2016) 160-165.
[2] Anes, V., Reis, L., De Freitas, M., On the assessment of multiaxial fatigue damage under variable amplitude loading, Frattura ed Integrita Strutturale, 10(37) (2016) 124-130.
[3] Albinmousa, J., Investigation on parametric representation of proportional and nonproportional multiaxial fatigue responses, Frattura ed Integrita Strutturale, 10(37) (2016) 94-100.
[4] Mazanova, V., Polak, J., Skorik, V., Kruml, T., Multiaxial elastoplastic cyclic loading of austenitic 316L Steel, Frattura ed Integrita Strutturale, 11(40) (2017) 162-169.
[5] Pook, L.P., Berto, F., Campagnolo, A., Lazzarin, P., Coupled fracture mode of a cracked disc under anti-plane loading, Eng. Fract. Mech., 128 (2014) 22-36.
[6] Kotousov, A., Berto, F., Lazzarin, P., Pegorin, F., Three dimensional finite element mixed fracture mode under anti-plane loading of a crack, Theor. Appl. Fract. Mech., 62(1) (2012) 26-33.
[7] Carpinteri, A., Spagnoli, A., Multiaxial high-cycle fatigue criterion for hard metals, Int. J. Fatigue, 23 (2001) 135-145.
[8] Carpinteri, A., Spagnoli, A., Vantadori, S., Multiaxial fatigue life estimation in welded joints using the critical plane approach, Int. J. Fatigue, 31 (2009) 188-196.
[9] Łagoda, T., Macha, E., Bedkowski, W., A critical plane approach based on energy concepts: application to biaxial random tension-compression high-cycle fatigue regime, Int. J. Fatigue, 21 (1999) 431-443.
[10] Ye, D., Hertel, O., Vormwald, M., A unified expression of elastic–plastic notch stress–strain calculation in bodies subjected to multiaxial cyclic loading, Int. J. Solids Struct., 45 (2008) 6177-6189.
[11] Nieslony, A., Sonsino, C.M., Comparison of some selected multiaxial fatigue assessment criteria, LBF Report No. FB-234 (2008).

[12] Ayatollahi, M.R., Razavi, S.M.J., Yahya, M.Y., Mixed mode fatigue crack initiation and growth in a CT specimen repaired by stop hole technique, Eng. Fract. Mech. 145 (2015) 115-127.
[13] Ayatollahi, M.R., Razavi, S.M.J., Chamani, H.R., Fatigue Life Extension by Crack Repair Using Stop-hole Technique under Pure Mode-I and Pure mode-II Loading Conditions, Procedia Eng., 74 (2014) 18–21.
[14] Ayatollahi, M.R., Razavi, S.M.J., Chamani, H.R., A numerical study on the effect of symmetric crack flank holes on fatigue life extension of a SENT specimen, Fatigue Fract. Eng. Mater. Struct., 37(10) (2014) 1153-1164.
[15] Ayatollahi, M.R., Razavi, S.M.J., Rashidi Moghaddam, M., Berto, F., Mode I fracture analysis of Polymethylmetacrylate using modified energy—based models, Phys. Mesomech. 18(5) (2015) 53-62.
[16] Ayatollahi, M.R., Rashidi Moghaddam, M., Razavi, S.M.J., Berto, F., Geometry effects on fracture trajectory of PMMA samples under pure mode-I loading, Eng. Fract. Mech., 163 (2016) 449–461.
[17] Ayatollahi, M.R., Razavi, S.M.J., Sommitsch, C., Moser, C., Fatigue life extension by crack repair using double stop-hole technique, Mater. Sci. Forum 879 (2017) 3-8.
[18] Rashidi Moghaddam, M., Ayatollahi, M.R., Razavi, S.M.J., Berto, F., Mode II Brittle Fracture Assessment Using an Energy Based Criterion, Phys. Mesomech. (in press).
[19] Razavi, S.M.J., Ayatollahi, M.R., Sommitsch, C., Moser, C., Retardation of fatigue crack growth in high strength steel S690 using a modified stop-hole technique, Eng. Fract. Mech. 169 (2017) 226–237.
[20] Pook, L.P., Sharples, J.K., The mode III fatigue crack growth threshold for mild steel, Int. J. Fract., 15 (1979) R223-R226.
[21] Pook, L.P., The fatigue crack direction and threshold behaviour of mild steel under mixed mode I and III loading, Int. J. Fatigue, 7 (1985) 21-30.
[22] Tong, J., Yates, J.R., Brown, M.W., Some aspects of fatigue thresholds under mode III and mixed mode and I loadings, Int. J. Fatigue, 18 (1986) 279-285.
[23] Christopher, C.J., James, M.N., Patterson, E.A., Tee, K.F., Towards a new model of crack tip stress fields, Int. J. Fract. 148 (2007) 361–371.
[24] Lin, B., Mear, M.E., Ravi-Chandar, K., Criterion for initiation of cracks under mixed-mode I + III loading, Int. J. Fract. 165 (2010) 175-188.
[25] Atzori, B., Berto, F., Lazzarin, P., Quaresimin, M., Multiaxial fatigue behaviour of a severely notched carbon Steel, Int. J. Fatigue, 28 (2006) 485-493.
[26] Berto, F., Lazzarin, P., Yates, J., Multiaxial fatigue of V-notched steel specimens: a non-conventional application of the local energy method, Fatigue Fract. Eng. Mater. Struct. 34 (2011) 921–943.
[27] Berto, F., Lazzarin, P., Fatigue strength of structural components under multi-axial loading in terms of local energy density averaged on a control volume, Int. J. Fatigue, 33 (2011) 1055-1065.
[28] Gallo, P., Berto, F., Glinka, G Generalized approach to estimation of strains and stresses at blunt V-notches under non-localized creep, Fatigue Fract. Eng. Mater. Struct, 39 (2016) 292-306.